



This is a repository copy of *Physicochemical analysis of initial adhesion and biofilm formation of Methanosarcina barkeri on polymer support material.*

White Rose Research Online URL for this paper:  
<http://eprints.whiterose.ac.uk/99099/>

Version: Accepted Version

---

**Article:**

Nguyen, V., Karunakaran, E., Collins, G. et al. (1 more author) (2016) Physicochemical analysis of initial adhesion and biofilm formation of *Methanosarcina barkeri* on polymer support material. *Colloids and Surfaces B: Biointerfaces*, 143. pp. 518-525. ISSN 0927-7765

<https://doi.org/10.1016/j.colsurfb.2016.03.042>

---

Article available under the terms of the CC-BY-NC-ND licence  
(<https://creativecommons.org/licenses/by-nc-nd/4.0/>).

**Reuse**

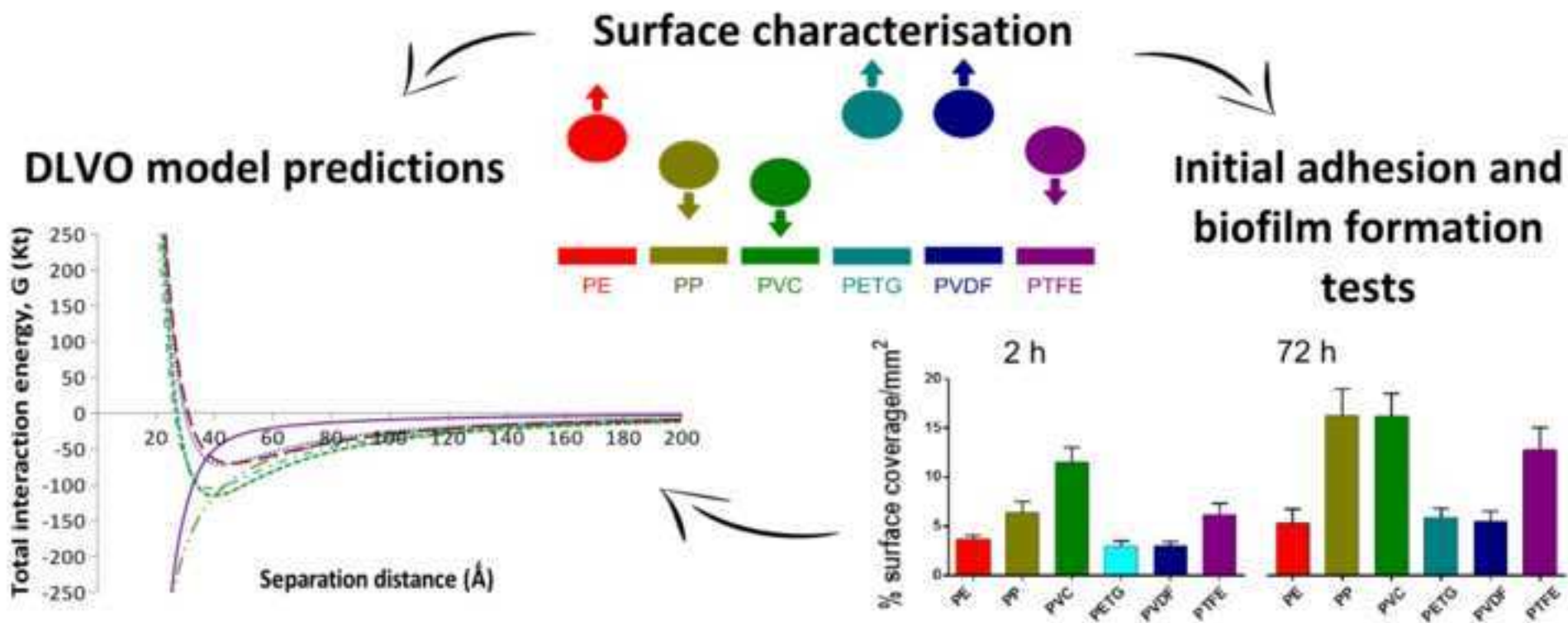
This article is distributed under the terms of the Creative Commons Attribution-NonCommercial-NoDerivs (CC BY-NC-ND) licence. This licence only allows you to download this work and share it with others as long as you credit the authors, but you can't change the article in any way or use it commercially. More information and the full terms of the licence here: <https://creativecommons.org/licenses/>

**Takedown**

If you consider content in White Rose Research Online to be in breach of UK law, please notify us by emailing [eprints@whiterose.ac.uk](mailto:eprints@whiterose.ac.uk) including the URL of the record and the reason for the withdrawal request.



[eprints@whiterose.ac.uk](mailto:eprints@whiterose.ac.uk)  
<https://eprints.whiterose.ac.uk/>



## Highlights

- Of the six materials tested *Methanosarcina barkeri* selectively adheres to polytetrafluoroethylene (PTFE), polypropylene (PP) and polyvinyl chloride (PVC)
- The best support materials for initial adhesion after 2 h also performed best after 72 h.
- xDLVO model predictions correlated with experimental adhesion results.
- Applicability of the xDLVO model in identifying support materials for selective attachment of *M. barkeri*.

## Physicochemical analysis of initial adhesion and biofilm formation of *Methanosarcina barkeri* on polymer support material

Vi Nguyen<sup>a</sup>, Esther Karunakaran<sup>a</sup>, Gavin Collins<sup>b</sup>, Catherine A. Biggs<sup>a\*</sup>

<sup>a</sup>Department of Chemical and Biological Engineering, University of Sheffield, Sheffield, S1 3JD. United Kingdom.

<sup>b</sup>Microbiology, School of Natural Sciences, NUI Galway, University Road, Galway, Ireland.

\* Corresponding author:

Catherine Biggs,

Department of Chemical and Biological Engineering, University of Sheffield, Sheffield, S1 3JD. United Kingdom.

Tel: (+44)114 222 7510; Fax: (+44)114 222 7501

Email: c.biggs@sheffield.ac.uk

### Highlights

- Of the six materials tested *Methanosarcina barkeri* selectively adheres to polytetrafluoroethylene (PTFE), polypropylene (PP) and polyvinyl chloride (PVC)
- The best support materials for initial adhesion after 2 h also performed best after 72 h.
- xDLVO model predictions correlated with experimental adhesion results.
- Applicability of the xDLVO model in identifying support materials for selective attachment of *M. barkeri*.

### Abstract

The retention of selective biofilms of *Methanosarcina* species within anaerobic digesters could reduce start-up times and enhance the efficiency of the process in treating high-strength domestic sewage. The objective of the study was to examine the effect of the surface characteristics of six common polymer support materials on the initial adhesion of the model methanogen, *Methanosarcina barkeri*, and to assess the potential of these support materials as selective biofilm carriers. Results from both the initial adhesion tests and extended DLVO (xDLVO) model correlated with each other, with PVC (12% surface coverage/mm<sup>2</sup>), PTFE (6% surface coverage/mm<sup>2</sup>), and PP (6% surface coverage/mm<sup>2</sup>), shown to be the better performing support materials for initial adhesion, as well as subsequent biofilm formation by *M. barkeri* after 72 h. These three support materials Experimental results showed that the type of material strongly influenced the extent of adhesion from *M. barkeri* ( $p < 0.0001$ ), and the xDLVO model was able to explain the results in these environmental conditions. Therefore, DLVO physicochemical forces were found to be influential on the initial adhesion of *M. barkeri*. Scanning electron microscopy suggested that production of extracellular polymeric substances (EPS) from *M. barkeri* could facilitate further biofilm development. This study highlights the potential of using the xDLVO model to rapidly identify suitable materials for the selective adhesion of *M. barkeri*, which could be beneficial in both the start-up and long-term phases of anaerobic digestion.

Keywords: *Methanosarcina barkeri*, DLVO model, physicochemical, initial adhesion, biofilm formation, support material

## Introduction

Anaerobic digestion is considered to be a low-cost and ecologically sustainable technology that has already shown great success in treating and harnessing two valuable end-products from waste biomass: biogas, a renewable energy source, and a nitrogen and phosphorous-rich digestate[1]. It is a natural process in which organic material is converted into methane and carbon dioxide by a highly specialised consortium of microorganisms in an oxygen-free environment. Complex macromolecules are broken down into simple one-carbon substrates, particularly acetate, for methanogenic archaea to convert into methane[2].

The principal methanogens involved in anaerobic digestion are slow growing compared to the other members of the consortium, and have extremely specialised metabolic pathways and environmental conditions for producing methane[3]. As a result, anaerobic digestion is hindered by long start-up times, inefficient bio-product productivity and low quality biogas[4], due to the frequent washout of these slower-growing methanogenic archaea from reactors and their sensitivity towards various operational and environmental fluctuations, such as pH, temperature and loading rate[5–7]. The vulnerability of the methanogenic consortium is one of the key limitations in the anaerobic digestion process[8].

However, methanogens from the genus *Methanosarcina* have been identified as being one of the more robust methanogens of the methanogenic consortium. Compared to the other methanogens, they are able to tolerate various environmental and operational stressors owing to their large cell size, unique mode of aggregated growth and use of various metabolic pathways for methane production[3,8,9].

As such, the selective retention of an active biomass of robust *Methanosarcina* within anaerobic digesters is desirable to reduce start-up times for the treatment of high strength domestic sewage. The poor global management of this waste poses serious health and environmental risks in many parts of the world[10,11]. Previous studies have reported a shift in the microbial community to mainly *Methanosarcina* sp. in dry anaerobic digestion processes, which characteristically digest high-solid waste substrates[8,12], as well as in ‘stressed’ reactors with high ammonia levels[13] and wide fluctuations in temperature and pH[8]. Having a high active biomass of *Methanosarcina* holds promise for heavy duty biomethanation for future biotechnological applications.

Recent studies have suggested a strong preferential attachment of methanogenic archaea to specific support materials within anaerobic digesters depending on the physicochemical characteristics of both the abiotic and microbial surfaces, such as surface charge [14], surface free energy [15] and hydrophobicity [7,15,16]. The nature of the support material has been strongly linked to improving the efficiency and performance of the anaerobic digestion process [1,7]. However, our knowledge of archaeal biofilms is limited, and the mechanism of initial adhesion between methanogenic archaea and support materials within anaerobic digesters is not well understood.

Microbial initial adhesion has been described in past studies using the extended Derjaguin-Landau-Verwey-Overbeek theory (xDLVO) [17], where particle adhesion is described in terms of the interfacial Lifshitz-van der Waals, electrostatic double layer and Lewis acid-base interactions as a function of separation distance, and are calculated from experimental surface parameter

measurements [18]. To our knowledge, this has not been applied for understanding the adhesion behaviour of key methanogenic species in fixed-film anaerobic digesters.

The objective of the present study was therefore to examine the effect of the surface characteristics of six common polymer support materials on the initial adhesion of *M. barkeri*, and to assess the potential of these support materials as selective biofilm carriers. Specifically, the focus was on the effect of high ionic strength and neutral pH on initial adhesion, characteristics both typical of domestic sewage. The findings from this study will not only provide a framework in which to better describe and understand the initial adhesion and biofilm formation of *M. barkeri*, but will also aid in the selection of support materials for the targeted immobilization of key *Methanosarcina* sp. to enhance the start-up of anaerobic digesters.

## **Materials and Methods**

### **Strain information, medium and inoculum preparation**

Cultures of the archaeal strain *Methanosarcina barkeri* DSM 800 were obtained from DSMZ (DSMZ, Braunschweig, Germany). New stock cultures were maintained by monthly subculture from a frozen glycerol stock using a 10% v/v inoculum in DSM 120 medium (pH 6.8)[19], consisting of dibasic potassium phosphate (0.35g), potassium dihydrogen phosphate (0.23g), ammonium chloride (0.5g), magnesium sulphide heptahydrate (0.5g), calcium chloride dehydrate (0.25g), sodium chloride (2.25g), iron(II) sulphate heptahydrate (2mg), trace element solution (1ml), yeast extract (2g) and casitone (2g). 50 ml of medium was added to 120 ml serum bottles and sparged with 100% nitrogen gas (N<sub>2</sub>) before being sealed with butyl rubber tops and autoclaved. Additional media components (methanol, cysteine-hydrochloride, sodium sulphide nonahydrate and sodium bicarbonate) were prepared in the same way, by flushing with 100% N<sub>2</sub> gas before being sealed and autoclaved. These were added to bottles of sterile DSM 120 medium before inoculation using an aseptic syringe method. All inoculations and subculturing were performed in an anaerobic chamber (PLAS-LAB Simplicity 888, PLAS-LABS, U.S.A.).

Cultures were incubated at 37°C for 4 days and growth was monitored by optical density measurements at 600 nm (OD<sub>600</sub>). To maintain reproducibility of results and to avoid phenotypic drift from repetitive culturing, experiments were started from maintained stock cultures and were subcultured no more than 3 times.

### **Support material preparation**

Six different support materials were used, consisting of common engineering plastics chosen for their low cost, durability and availability: polyethylene (PE), polypropylene (PP), polyvinyl chloride (PVC), polyvinylidene fluoride (PVDF), polyethylene terephthalate glycol (PETG) and polytetrafluoroethylene (PTFE) (Engineering & Design Plastics Ltd., Cambridge, U.K.). Each plastic was cut into 1 x 1 cm square coupons for the initial adhesion and biofilm formation experiments, and into 1.5 cm x 6 cm coupons for streaming potential and contact angle measurements.

The plastic coupons were cleaned with 70 % ethanol to remove grease on the surface before being submerged into a 2% v/v PCC-54 detergent solution (Fisher Scientific, U.K.), and subjected to a water sonication bath for 5 minutes. The coupons were then rinsed several times with ultrapure water until they stopped foaming. They were dried inside a laminar flow cabinet and further UV-sterilised for 3 hours, before being stored in sterile tubes for future use.

### **Contact angle measurement**

Contact angles of *M. barkeri* and the support materials were measured using the sessile drop technique using a tensiometer (Attension Theta Lite, Biolin Scientific, Sweden) and 3 probe liquids of different polarity and with known surface energy [16,20,21]. These liquids were ultrapure water, diiodomethane (Sigma-Aldrich, U.K.) and formamide (Sigma-Aldrich, U.K.). Measurements were carried out at room temperature (22°C).

Coupons with dimensions of 1.5 cm x 6 cm were prepared for each of the support materials. Results reported are for 3 replicate coupons and a droplet of each probe liquid deposited onto a randomly selected location on the surface of each support material coupon.

*M. barkeri* cells were harvested at mid-exponential phase, as monitored by optical density measurements at 600 nm (OD<sub>600</sub>), and centrifuged at 6000 x g for 5 minutes and rinsed twice with 100 mM potassium chloride solution (KCl) at pH 7. Using a vacuum pump to provide a negative pressure, washed cells were filtered onto a 0.45 µm pore nitrocellulose filter membrane (Millipore, U.S.A.) to obtain an even lawn of microbial cells [21]. A drying time of 20 minutes was used for all contact angle measurements. Results reported are for 3 biological replicates and a droplet of each liquid deposited onto a randomly selected location on the microbial lawn.

### Calculation of surface free energy components

The surface free energy of a substance is the additive effect of Lifshitz-van der Waals ( $\gamma^{LW}$ ) and acid-base ( $\gamma^{AB}$ ) components [16,20,22]. Furthermore, the polar AB component consists of electron-donating ( $\gamma^+$ ) and electron-accepting ( $\gamma^-$ ) parameters. The extended Young equation was used to determine these surface free energy components for *M. barkeri* and the support materials [16]:

$$(1 + \cos \theta)\gamma_l = 2 \left( \sqrt{\gamma_s^{LW}\gamma_l^{LW}} + \sqrt{\gamma_s^+\gamma_l^-} + \sqrt{\gamma_s^-\gamma_l^+} \right) \quad (1)$$

where  $\theta$  is the contact angle of the three probe solutions on the surface,  $\gamma_l$  is the surface energy of the probe liquids, and  $\gamma^{LW}$ ,  $\gamma^+$ ,  $\gamma^-$  are the Lifshitz-van der Waals, electron acceptor and electron donor parameters of the solids (s), or *M. barkeri* and the support materials in this case.

The total contribution of the polar AB component of the surface free energy was calculated as the geometric mean of the electron-donating ( $\gamma^-$ ) and electron-accepting ( $\gamma^+$ ) parameters [16,20,22]:

$$\gamma^{AB} = 2\sqrt{\gamma^+\gamma^-} \quad (2)$$

### Zeta potential analysis

Electrokinetic measurements were made to analyse the streaming potential of each support material, using an EKA Electrokinetic Analyser (Anton Parr GmbH, Austria) at the School of Chemical and Process Engineering, University of Leeds, U.K.

Coupons of the support materials with dimensions of 1.5 cm x 6 cm were placed in a rectangular measuring cell between two Ag/AgCl electrodes. A 100 mM KCl solution at pH 7 was circulated around the system and inside the streaming channel of the measuring cell, with a rinse pressure of 300 mbar. This ionic solution was used to model the characteristics of a high strength

domestic sewage typically found in arid regions with low household water consumption[23]. The zeta potential was calculated from the streaming potential by the software based on the Smoluchowski equation[24].

The electrophoretic mobility (EPM) of *M. barkeri* was measured using phase amplitude light scattering (ZetaPALS, Brookhaven Instruments, U.K.) in 100 mM KCl solution, adjusted to pH 7. Cells were harvested at mid-exponential phase, washed and resuspended in 100 mM KCl solution at pH 7. An electric field of 2.5 V cm<sup>-1</sup> and a frequency of 2.0 Hz were used to measure the EPM, as these settings have successfully been used in previous studies of biosystems [25]. The zeta potentials of *M. barkeri* were calculated from EPM measurements using the Smoluchowski equation. Results are reported as an average of 20 cycles, 3 biological replicates and 3 independent experiments.

### xDLVO energy profiles

The total interaction energy between *M. barkeri* and the support materials in a 100 mM KCl, pH 7 aqueous environment was determined using the xDLVO model. The model is based on the assumption of spherical particles, which was in accordance with the spherical cell morphology of *M. barkeri*. The sphere-flat plate equations were used in the xDLVO model[16] to model the interaction between the spherical microbial cells and flat plate dimensions of the polymer support materials.

The Lifshitz-van der Waals and acid-base model (LW-AB) developed by Van Oss and co-workers [26] forms the basis of the xDLVO model, and is used to determine the free energy of interaction between microbial and abiotic surfaces ( $G^{TOT}$ ) over a separation distance,  $H$ . It takes into account the additive effect of the Lifshitz-van der Waals (LW), electrostatic double layer (EL) and Lewis acid-base (AB) free energy of interaction as a function of separation distance ( $H$ )[16]:

$$G^{TOT}(H) = G^{LW}(H) + G^{EL}(H) + G^{AB}(H) \quad (3)$$

The following equations were used to calculate the LW, EL and AB interaction energies[16,20]:

$$G^{LW}(H) = -\frac{A}{12} \left[ \frac{2a(H+a)}{H(H+2a)} - \ln \left( \frac{H+2a}{H} \right) \right] \left( \frac{1}{1+1.77(2\pi H/\lambda)} \right) \quad (4)$$

Where  $a$  is the radius of *M. barkeri* cells which was assumed to be 1  $\mu\text{m}$ [9] and  $\lambda$  is the correlation length of molecules in liquid, which was taken to be 0.6 nm for hydrophilic bacteria[16,22,27] and  $A$  is the Hamaker constant, calculated as:

$$A = -12\pi h_0^2 \Delta G_{adh}^{LW} \quad (5)$$

The EL interaction energy was calculated as follows[16]:

$$G^{EL}(H) = \pi \epsilon \alpha (\zeta_1^2 + \zeta_2^2) \left[ \frac{2\zeta_1 \zeta_2}{\zeta_1^2 + \zeta_2^2} \ln \left( \frac{1+e^{-kH}}{1-e^{-kH}} \right) + \ln(1 - e^{-2kH}) \right] \quad (6)$$

where  $\zeta$  is the zeta potential of *M. barkeri* and the support material surfaces and assumed to be the same as the surface potential,  $\epsilon$  is the electrical permittivity of the medium ( $8.854 \times 10^{-12} \text{ C}^2 \text{ J}^{-1} \text{ m}^{-1}$ )[22,27],  $H$  is the separation distance and  $k$  is the double layer thickness, calculated as[16]:

$$k = 0.3281\sqrt{I}^{-1} \quad (7)$$

where  $I$  is the ionic strength in terms of molarity.

$$G^{AB}(H) = 2\pi a\lambda \Delta G^{AB} e^{[(d_0-H/\lambda)]} \quad (8)$$

where  $d_0$  is the minimum separation distance between two surfaces (4.57 Å at high ionic strength)[16].

### Initial adhesion

Clean coupons (1 x 1 cm) of each of the support materials were secured into wells of a sterile 24 well plate (Corning Costar, U.S.A.) using 10 µl of silicone sealant (Aquarium Sealant, King British, U.K.), which has been used as a non-toxic adhesive in previous static biofilm studies [28]. Experimental plates were prepared in a laminar flow cabinet and UV-sterilised for 3 h before being placed in an anaerobic chamber for at least 48 h prior to the initial adhesion experiment to remove all residual traces of oxygen from plates and coupons.

Cells of mid-exponential phase *M. barkeri* cultures were harvested by centrifugation (Heraeus Megafuge 16, Thermo Scientific, U.S.A.) at 6000 x g for 5 minutes in sterile microcentrifuge tubes inside an anaerobic chamber. Cell pellets were rinsed twice and resuspended in 100 mM KCl solution at pH 7.

Wells of prepared 24 well plates were filled with 2 ml of cell suspension of *M. barkeri* with an adjusted OD<sub>600</sub> of 0.3. Control wells contained clean plastic coupons in sterile 100 mM KCl, pH 7 solution only. Plates were incubated at room temperature (22°C) and gently shaken at 110 rpm in an incubating mini shaker inside the anaerobic chamber (VWR International, U.S.A.) for 2 h. This short duration was chosen to examine initial microbial adhesion and to prevent established biofilm formation from *M. barkeri*.

After 2 h, coupons were rinsed twice with anaerobically prepared 100 mM, pH 7 KCl and fixed with 4% paraformaldehyde solution (Sigma-Aldrich, U.K.) for 15 minutes inside the anaerobic chamber. Thereafter, coupons were rinsed twice with phosphate-buffered saline (PBS) consisting of 8g NaCl, 200mg KCl, 1.44g Na<sub>2</sub>HPO<sub>4</sub> and 240mg KH<sub>2</sub>PO<sub>4</sub>. Fixed coupons were stored at 4°C in PBS for future microscopic imaging.

### Biofilm formation

Cells of mid-exponential phase *M. barkeri* cultures were washed and harvested as described earlier and finally resuspended in DSM 120 anaerobic medium at pH 7. The biofilm assay was prepared using the same experimental conditions and in the same 24 well plates as used for the initial adhesion assay, except that adhesion occurred over a duration of 72 h at 37°C.

Thereafter, coupons were rinsed twice with anaerobically prepared 100 mM KCl at pH 7 and fixed with 4% paraformaldehyde solution (Sigma-Aldrich, U.K.) for 15 minutes inside the anaerobic chamber. Coupons were rinsed twice with PBS and stored at 4°C in PBS.

### Epifluorescence microscopy

Coupons with fixed biofilm were labeled with 1 µg/ml DAPI (diamidino-4,6- phenyllindol-2 dichlorhydrate) solution (Sigma-Aldrich, U.K.) for 10 minutes at room temperature in the dark, and rinsed twice with PBS.

Epifluorescence microscopy was used to ascertain the area covered by adhered *M. barkeri* cells. Acquisition was facilitated with a Leica AF6000 inverted microscope (Leica Microsystems GmbH, Germany) attached to a computer with a magnification of 100 in order to obtain a representative surface coverage of coupons. 20 microscopic fields (1 mm<sup>2</sup> per field) were randomly selected for each coupon and measured for surface area coverage. Images were analysed with the ImageJ software to calculate the average percentage of area covered by cells after 2 h and 72 h.

### **Scanning electron microscopy (SEM)**

To visualize cell adhesion after 2 h and 72 h, a parallel experiment was run alongside the initial adhesion and biofilm formation tests, using the exact same experimental conditions, in which adhering cells on the support materials were viewed under a scanning electron microscope (Electron Microscopy Unit, University of Sheffield, U.K.).

Coupons of each support material from both adhesion assays were removed from cell suspensions into sterile 24 well plates and rinsed twice with sterile, anaerobically prepared 100 mM KCl inside an anaerobic chamber. Coupons were then fixed with 2% glutaraldehyde in 0.1 M sodium cacodylate buffer (Sigma-Aldrich, U.K.) at 4°C for 16 hours. Secondary fixation was carried out in 2% osmium tetroxide solution (Sigma-Aldrich, U.K.) before fixed samples were dehydrated through a graded series of 75% to 100% ethanol. Fixed samples were sputter-coated with gold before mounted onto stubs and viewed using a Philips XL-20 scanning electron microscope (Philips, Netherlands) at an accelerating voltage of 20 kV.

### **Statistical analysis**

Statistical analysis was performed using GraphPad Prism (GraphPad Software, Inc., U.S.A.). The Brown-Forsythe test was used to determine statistical differences between group variances. The non-parametric Kruskal-Wallis test was used to compare percentage adhesion data after 2 h and 72 h between the support materials, followed by *post-hoc* analysis using Dunn's multiple comparison test.

## **Results**

### **Surface characterisation**

#### *Contact angle measurement*

The contact angles of water, formamide and diiodomethane on the surfaces of *M. barkeri* and the support materials are shown in Table 1, and were used to calculate surface free energy. Water contact angles were used as an indication of hydrophobicity[20,29].

The support materials each had similarly low surface free energies. These ranged from 28 mJ.m<sup>-2</sup> to 48 mJ.m<sup>-2</sup>, with PTFE having the lowest total surface free energy and also having the most hydrophobic surface, with a high water contact angle of 116°. On the other hand, PVC possessed the highest surface free energy and was the most hydrophilic surface with a comparatively lower water contact angle of 72°. In addition to PTFE, PP also possessed a hydrophobic surface, whereas the remaining support materials had hydrophilic surfaces.

All support materials had a van der Waals component ( $\gamma^{LW}$ ) that far exceeded the polar acid-base component ( $\gamma^{AB}$ ). Van Oss et al. (1988)[26] demonstrated a propensity for organic materials, such as plastics, to have a  $\gamma^{LW}$  of  $40 \text{ mJ}\cdot\text{m}^{-2}$ , which is in accordance with these results.

On the other hand, *M. barkeri*, having a water contact angle of  $8^\circ$ , had the most hydrophilic surface compared to the support materials. Most microorganisms possess hydrophilic surfaces, with water contact angles less than  $60^\circ$ [20,29]. In this study, *M. barkeri* also possessed a more energetic surface than the support materials, with a total surface free energy of  $57 \text{ mJ}\cdot\text{m}^{-2}$ .

#### *Zeta potential analysis*

The zeta potentials of the support materials were determined from streaming potential measurements using the Smoluchowski equation. PVC had the least negative zeta potential at 100 mM KCl and pH 7 (-5 mV), closely followed by PTFE with -6 mV. On the other hand, PVDF had the most negative surface zeta potential with -39 mV.

All solid surfaces exhibited negative zeta potentials, indicating negative surface charge under the conditions tested. *M. barkeri* also possessed a relatively negative zeta potential of -20 mV at 100 mM KCl and pH 7.

#### **xDLVO energy profiles**

Assumptions for *M. barkeri* with regards to its morphology and surface charge were made when using the xDLVO model. *M. barkeri* has a large spherical shape of approximately  $0.5\text{-}3\mu\text{m}$  in size[9], which falls within the remit of the equations for the xDLVO model[18]. Zeta potentials calculated from electrophoretic mobility and streaming potential measurements using the Smoluchowski equation were used instead of surface potentials, as this cannot be experimentally determined.

The total interaction energy of adhesion as determined by the xDLVO model between *M. barkeri* and the support materials was calculated as a function of separation distance, in 100 mM KCl at pH 7. For ease of presentation, the Lifshitz-van der Waals, electrostatic double layer and acid-base interaction energies are also illustrated for each support material with *M. barkeri* (see Supplementary Material).

These predicted energy profiles demonstrate that at small separation distances, repulsion is predicted between *M. barkeri* and all the support materials except for PTFE and PP, as a result of repulsive short-range  $G^{AB}$  (Fig.S1). These polar interactions create an energy barrier at the surface and prevent the irreversible adhesion of *M. barkeri* to PE, PETG, PVDF and PVC. However, these repulsive forces only operate at small separation distances of  $30 \text{ \AA}$ .

A secondary minimum is present at longer separation distances corresponding to  $30 \text{ \AA}$  from the substratum for PE, PETG and PVC and  $45 \text{ \AA}$  for PVDF (Fig.1). At these separation distances, approaching cells are predicted to reversibly attach to these support materials, but irreversible adhesion is not possible due to the energy barrier. The depths of the secondary minima suggests that irreversible adhesion is more likely to spontaneously occur on PVC with a net attractive interaction energy at secondary minimum of approximately 120 kT, whereas PVDF exhibited the lowest net attractive interaction energy at secondary minimum of approximately 50 kT (Fig.1).

Repulsive electrostatic  $G^{EL}$  forces were present for all combinations of *M. barkeri* and support material. Strong, long-range  $G^{EL}$  interactions were predicted between *M. barkeri* and PVDF and PE at 70 Å and 50 Å respectively from the substratum (Fig.S1), due to their highly charged surfaces (Table 1). The strength of the  $G^{EL}$  forces was less dominant for PVC and PTFE in particular, due to their low charged surfaces (Table 1) and a reduced electrostatic repulsion. Conversely, all combinations of *M. barkeri* and support material exhibited attractive  $G^{LW}$  interactions (Fig.S1).

PP and PTFE were the only support materials to exhibit both attractive  $G^{LW}$  and  $G^{AB}$  interactions (Fig.S1). These superseded the repulsive short-range  $G^{AB}$  interactions, resulting in a strong net attractive force between microbial and abiotic substrata. The xDLVO model predicted irreversible adhesion of *M. barkeri* cells to these surfaces.

All microbial and abiotic support materials had polar surfaces (Table 1), and the xDLVO model showed that acid-base interactions played a large part in attraction or repulsion.

### **Initial adhesion**

The initial adhesion of *M. barkeri* to the support materials after 2 h in 100 mM KCl at pH 7 was quantified in terms of the percentage of the surface area covered by adhering cells per  $\text{mm}^2$  using epifluorescence microscopy (Fig.2a).

*M. barkeri* exhibited different abilities to attach to the support materials after 2 h, with the type of material strongly influencing the extent of cell adhesion ( $p < 0.0001$ , Kruskal-Wallis test).

The percentage of surface coverage varied across all support materials, with PVC performing best in promoting the initial adhesion of *M. barkeri*, with 12% of the surface area/ $\text{mm}^2$  colonized by cells after 2 h. PTFE and PP also promoted a high percentage surface coverage from cells of *M. barkeri*.

However, PETG, PVDF and PE possessed the poorest surfaces for initial colonization from *M. barkeri*, exhibiting  $< 5\%$  surface coverage per  $\text{mm}^2$ . There was no significant difference in the level of initial adhesion from *M. barkeri* to these three support materials ( $p > 0.05$ , Kruskal-Wallis and Dunn's multiple comparison test). However, there was a marked difference between these support materials and PVC, PP and PTFE in their ability to promote initial attachment from *M. barkeri* ( $p < 0.05$ , Kruskal-Wallis and Dunn's multiple comparison test).

### **Biofilm formation**

The biofilm capability of *M. barkeri* to the support materials was tested after 72 h in basal media. Results showed different levels of adhesion to the support materials within this time frame (Fig.2b), with the type of material strongly influencing the extent of cell adhesion ( $p < 0.0001$ , Kruskal-Wallis test).

Similar to the findings from the initial adhesion test, the surfaces of PVC, PP and PTFE were shown to promote biofilm formation from *M. barkeri* after 72 h, with more than 12% of the surface covered by cells per  $\text{mm}^2$  (Fig.2b). There was not a significant difference in the level of adhesion between these three support materials after this time frame ( $p > 0.05$ , Kruskal-Wallis and Dunn's multiple comparison test).

The poorest surfaces for biofilm formation were provided by PETG, PVDF and PE. There was a marked difference between these support materials and PVC, PP and PTFE in the level of biofilm formed by *M. barkeri* after 72 h ( $p < 0.05$ , Kruskal-Wallis and Dunn's multiple comparison test).

### Scanning electron microscopy

SEM imaging was used to qualitatively analyse the physical properties and adhesion behaviour of *M. barkeri* on the different support materials after 2 h in 100 mM KCl and 72 h in basal media. The initial adhesion of *M. barkeri* to the support materials proceeded as a random attachment of cells in isolated patchy areas after 2 h (Fig.S2).

After 72 h in basal media, SEM images show different cell morphologies and the presence of additional material on the surfaces of PVC and PTFE in particular (Fig.3), which could be attributed to secreted extracellular polymeric material (EPS). In comparison, the other support materials were more sparsely covered by cells of *M. barkeri* after 72 h, particularly PETG and PVDF.

### Discussion

Biofilms play an essential role in biological wastewater treatment processes. With initial adhesion being such an important precursor to biofilm formation, it is surprising that our understanding of the mechanisms underlying these processes from key methanogenic species in the anaerobic digestion process is still lacking. Past studies have demonstrated that the use of support materials have been used to great effect in promoting methanogenic biofilm formation within anaerobic digesters [2,7,15,30,31]. However, the challenge still remains in finding support materials that are selective for the retention of specific microbial groups [8], such as the metabolically diverse *Methanosarcina* species for heavy duty biomethanation.

Experimental adhesion results from this study showed that PVC, PTFE and PP possessed the best surfaces for initial adhesion and biofilm formation from *M. barkeri* (Fig.2) after 2 h in 100 mM KCl at pH 7, and after 72 h in basal media. To improve our understanding of the underlying mechanisms for the observed microbial adhesion behaviour, the xDLVO model was used to predict the interaction energies between microbial and abiotic substrata.

The predictions from the xDLVO model correlated closely with the experimental observations of high surface coverage of cells on PTFE and PP (Fig.2). According to the xDLVO model, PTFE and PP were the only support materials to exhibit both attractive  $G^{LW}$  and  $G^{AB}$  interactions (Fig.S1). These attractive interfacial interactions superseded the repulsive short-range  $G^{AB}$  interactions, resulting in a strong net attractive force between microbial and abiotic substrata. This highlights the important role that hydrogen bonding of the water molecules surrounding the interacting substrata has on the process of microbial adhesion to hydrophobic and low surface free energy materials[32]. Such surfaces are reported to have a better propensity in removing water from the area between two contacting substrata, therefore leading to a stronger level of microbial adhesion[33].

Additionally, the predicted irreversible adhesion of *M. barkeri* to PTFE can be described in terms of their polar parameters. *M. barkeri* has a strong electron-donating surface property,  $\gamma^-$ , which was predicted by the xDLVO model to be most attracted to the surface of PTFE, which possessed the highest  $\gamma^+$ (Table 1).

The xDLVO model was also able to account for the low percentage of surface coverage of cells to PE, PETG and PVDF after 2 h in 100 mM KCl, with experimental initial adhesion results in accordance with the depths of the predicted secondary minima (Fig.1). These results can be attributed to the highly negatively charged surfaces of *M. barkeri*, PVDF and PE (Table 1), which were predicted to generate strong repulsive  $G^{EL}$  interactions between *M. barkeri* and PVDF and PE at 70 Å and 50 Å respectively from the substratum (Fig.S1). These negative surface charges can be attributed to the presence of  $COO^-$  on the surfaces of these support materials, which has a negative zeta potential in the range of neutral pH [34].

Past studies using mixed methanogenic consortia found PVC to be a good support material for promoting high archaeal density within 2 h [7,15]. In fact, PVC and PP have been reported to being used as support materials in commercial wastewater treatment plants [15]. In this study also, it is interesting to note that out of all the polymer support materials tested, PVC fared best in promoting the selective attachment of *M. barkeri* in a single species adhesion test after 2 h in 100 mM KCl at pH 7. In order to explain this observation, it can be seen that PVC possessed the highest surface free energy and was the most hydrophilic surface with a water contact angle of 72° (Table 1). This is a result of PVC's high polar acid-base ( $\gamma^{AB}$ ) component, and can be attributable to its high electron-donating ( $\gamma^-$ ) nature (Table 1). Alternatively, *M. barkeri* exhibited a low water contact angle of 8° (Table 1) and strong hydrophilic properties that could be attributed to its unique methanochondroitin outer layer, which consists of glucuronic acid and acetylgalactosamine [9], both of which are hydrophilic in nature. It also has a high electron-donating component compared to its electron-accepting component, with a  $\gamma^-$  of 54 mJ.m<sup>-2</sup> (Table 1), indicating that *M. barkeri* has a strong polar surface [35,36]. This strong electron-donating surface property is typical of living surfaces [20]. It is possible that with PVC possessing such a polar surface with a high  $\gamma^{AB}$ , a greater number of interfacial acid-base interactions were established between the cells of *M. barkeri* and the surface of PVC, thus promoting a higher surface coverage from cells [37].

However, the xDLVO model predicted a secondary minimum between *M. barkeri* and PVC at a separation distance of 30 Å from the substratum, with a net attractive interaction energy of approximately 120 kT (Fig.1). This prediction deviated slightly from the observed high surface coverage of PVC by cells of *M. barkeri* (Fig.2).

Alternatively, from a biological viewpoint, non-DLVO forces such as polymer interactions could have accounted for the observed selective adhesion of *M. barkeri* to PVC. It is well understood that microorganisms possess and secrete various surface-based polymers, which can have a high affinity to different abiotic surfaces and facilitate attractive surface polymer interactions [24]. These polymer interactions play an important role in initial adhesion and are not accounted for in the xDLVO model [17]. Indeed, most species of *Methanosarcina* possess an external surface layer consisting of a thick polymeric network of methanochondroitin fibrils, which can extend 20-200 nm from the inner microbial surface layer and are responsible for cell-cell adhesion in this genus [9]. It is understood that surface structures are able to cross the repulsive energy barrier at separation distances of 20-100 nm from the substratum [17], allowing interacting surfaces to come into close contact when cells are retained in the secondary minimum [16]. Thus, such surface structures facilitate the transition into the primary minimum and a more irreversible attachment.

It is feasible that the highly polar surface of PVC combined with specific polymer interactions between the surface structures of *M. barkeri* and the surface of PVC could have promoted a more irreversible attachment in the primary minimum. Such deviations from the predictions of the DLVO model have been reported previously [24], and have been explained by the presence of microbial surface structures or chemical surface inhomogeneity [38].

The experimental results showed that the support materials promoting the highest affinity of adhering *M. barkeri* cells after 2 h in 100 mM KCl were also the best support materials for longer term attachment after 72 h in basal media (Fig.2); a media that is also highly ionic and neutral in pH [19]. Previous studies have also found this to be the case with mixed methanogenic consortia [7,15], indicating that the process of initial adhesion could be a critical factor for biofilm formation in methanogenic archaea.

SEM imaging suggested that the selective attachment of *M. barkeri* cells grown in basal media to PVC and PTFE in particular, could have been facilitated by the production of EPS within the 72 h time frame of this study (Fig.3). It has been reported that the placement of support materials within anaerobic reactors experience rapid attachment from mixed methanogenic consortia within a few hours [39,40], and can promote the early production of EPS [31].

The initial attachment of microbial cells to an abiotic surface is known to induce phenotypic and physiological changes in the cell, which can promote adhesion by the release of EPS [41]. This phenotypic cell change has been reported to occur earlier on hydrophobic and low surface free energy materials than on hydrophilic high surface free energy materials, and is a role of hydrophobicity [33]. This finding could explain the observed polymeric material on the surfaces of PVC and PTFE in the SEM images (Fig.3). However, further investigation would be needed to identify the composition of the additional biological material observed on the surfaces of PVC and PTFE in the SEM images, and their specific role in the biofilm formation process.

This study highlights the important role that the surface characteristics of support materials have in influencing adhesion. This holds true in this study, in which *M. barkeri* was shown to exhibit different abilities to attach to the six support materials, with the type of material strongly influencing the extent of attachment ( $p < 0.05$ ).

As the support materials that were predicted to promote the best cell adhesion from *M. barkeri* after 2 h correlated with the surface coverage results from both the initial adhesion and biofilm formation assays, this study highlights the potential of using the xDLVO model in a 2 h test to rapidly select the most suitable support materials for the selective immobilization of *M. barkeri* in high ionic strength and neutral pH aqueous environments.

## **Conclusions**

Overall, experimental results correlated closely to theoretical predictions. DLVO forces were shown to be mainly responsible for the initial attachment of *M. barkeri* to six polymer support materials in high ionic strength and neutral pH environments. *M. barkeri* was shown to adhere well to the most hydrophobic surfaces tested in this study, PTFE and PP. However, the model was less able to describe the highly selective initial adhesion of *M. barkeri* to PVC, but polymeric interactions could be a determining factor.

It is clear that the physicochemical properties of both the biotic and abiotic surface play a key role in initial adhesion and biofilm formation. This study highlights the importance of using polar and hydrophobic support materials for the selective attachment of *M. barkeri* in high ionic strength and neutral environments, and the use of the xDLVO model to rapidly screen suitable support materials for the selective attachment of *M. barkeri*.

### Acknowledgements

The authors wish to acknowledge the E-Futures Doctoral Training Centre and the UK Engineering and Physical Sciences Research Council for research funding (EP/J00538X/1; EP/E053556/1). Special thanks also to Michael Simmonds for assistance with the editing of all images in this article, and the University of Leeds for use of the streaming potential analyser.

### References

- [1] S.P. Singh, P. Prerna, Review of recent advances in anaerobic packed-bed biogas reactors, *Renew. Sustain. Energy Rev.* 13 (2009) 1569–1575.
- [2] N. Adu-Gyamfi, S.R. Ravella, P.J. Hobbs, Optimizing anaerobic digestion by selection of the immobilizing surface for enhanced methane production., *Bioresour. Technol.* 120 (2012) 248–55.
- [3] P. Weiland, Biogas production: current state and perspectives., *Appl. Microbiol. Biotechnol.* 85 (2010) 849–60.
- [4] W. Gong, H. Liang, W. Li, Z. Wang, Selection and evaluation of biofilm carrier in anaerobic digestion treatment of cattle manure, *Energy.* 36 (2011) 3572–3578.
- [5] T.R. Yadavika, S., Sreekrishnan, S. Kohli, V. Rana, Enhancement of biogas production from solid substrates using different techniques--a review., *Bioresour. Technol.* 95 (2004) 1–10.
- [6] T. Amani, M. Nosrati, T.R. Sreekrishnan, Anaerobic digestion from the viewpoint of microbiological, chemical, and operational aspects — a review, *Environ. Rev.* 18 (2010) 255–278.
- [7] F. Habouzit, J. Hamelin, G. Santa-Catalina, J.-P. Steyer, N. Bernet, Biofilm development during the start-up period of anaerobic biofilm reactors: the biofilm Archaea community is highly dependent on the support material., *Microb. Biotechnol.* 7 (2014) 257–64.
- [8] J. De Vrieze, T. Hennebel, N. Boon, W. Verstraete, Methanosarcina: the rediscovered methanogen for heavy duty biomethanation., *Bioresour. Technol.* 112 (2012) 1–9.
- [9] V. Milkevych, B.C. Donose, N. Juste-Poinapen, D.J. Batstone, Mechanical and cell-to-cell adhesive properties of aggregated Methanosarcina, *Colloids Surfaces B Biointerfaces.* 126 (2015) 303–312.
- [10] C.R. Lohri, L. Rodić, C. Zurbrügg, Feasibility assessment tool for urban anaerobic digestion in developing countries., *J. Environ. Manage.* 126 (2013) 122–31.
- [11] a M. Ingallinella, G. Sanguinetti, T. Koottatep, a Montanger, M. Strauss, The challenge of faecal sludge management in urban areas--strategies, regulations and treatment options., *Water Sci. Technol.* 46 (2002)

- [12] A. Abbassi-Guendouz, E. Trably, J. Hamelin, C. Dumas, J.P. Steyer, J.-P. Delgenès, et al., Microbial community signature of high-solid content methanogenic ecosystems., *Bioresour. Technol.* 133 (2013) 256–62.
- [13] O. Calli, B., Mertoglu, B., Inanc, B., Yenigun, Community changes during start-up in methanogenic bioreactors exposed to increasing levels of ammonia, *Environ. Technol.* 26 (2005) 85–91.
- [14] S.Z. Ahammad, R.J. Davenport, L.F. Read, J. Gomes, T.R. Sreekrishnan, J. Doling, Rational immobilization of methanogens in high cell density bioreactors, *RSC Adv.* 3 (2013) 774.
- [15] F. Habouzit, G. Gévaudan, J. Hamelin, J.-P. Steyer, N. Bernet, Influence of support material properties on the potential selection of Archaea during initial adhesion of a methanogenic consortium., *Bioresour. Technol.* 102 (2011) 4054–60.
- [16] P.K. Sharma, K. Hanumantha Rao, Adhesion of *Paenibacillus polymyxa* on chalcopyrite and pyrite: surface thermodynamics and extended DLVO theory, *Colloids Surfaces B Biointerfaces.* 29 (2003) 21–38.
- [17] M. Hermansson, The DLVO theory in microbial adhesion, *Colloids Surfaces B Biointerfaces.* 14 (1999) 105–119.
- [18] R. Bos, H.C. van der Mei, H.J. Busscher, Physico-chemistry of initial microbial adhesive interactions--its mechanisms and methods for study., *FEMS Microbiol. Rev.* 23 (1999) 179–230.
- [19] T. Nomura, A. Yoshihara, T. Nagao, H. Tokumoto, Y. Konishi, Effect of the surface characteristics of *Methanosarcina barkeri* on immobilization to support materials, *Adv. Powder Technol.* 18 (2007) 489–501.
- [20] H.C. van der Mei, R. Bos, H.J. Busscher, A reference guide to microbial cell surface hydrophobicity based on contact angles, *Colloids Surfaces B Biointerfaces.* 11 (1998) 213–221.
- [21] H.J. Busscher, A.H. Weerkamp, H.C. van der Mei, W.J. Antoon, A.W. Van Pelt, H.P. de Jong, et al., Measurement of the Surface Free Energy of Bacterial Cell Surfaces and Its Relevance for Adhesion, *Appl. Environ. Microbiol.* 48 (1984) 980–983.
- [22] G. Hwang, I.-S. Ahn, B.J. Mhin, J.-Y. Kim, Adhesion of nano-sized particles to the surface of bacteria: mechanistic study with the extended DLVO theory., *Colloids Surf. B. Biointerfaces.* 97 (2012) 138–44.
- [23] M. Henze, Y. Comeau, Wastewater Characterization, in: M. Henze, M.C.M. van Loosdrecht, G.A. Ekama, D. Brdjanovic (Eds.), *Biol. Wastewater Treat. Princ. Model. Des.*, IWA Publishing, London, UK, London, 2008: pp. 33–52.
- [24] A.T. Poortinga, R. Bos, W. Norde, H.J. Busscher, Electric double layer interactions in bacterial adhesion to surfaces, *Surf. Sci. Rep.* 47 (2002) 1–32.
- [25] C.A. Mukherjee, J., Karunakaran, E., Biggs, Using a multi-facteted approach to determine the changes in bacterial cell surface properties influenced by a biofilm lifestyle, *Biofouling.* 28 (2012) 1–14.

- [26] C.J. Van Oss, M.K. Chaudhury, R.J. Good, Interfacial Lifshitz-van der Waals and polar interactions in macroscopic systems, *Chem. Rev.* 88 (1988) 927–941.
- [27] B. Li, B.E. Logan, Bacterial adhesion to glass and metal-oxide surfaces., *Colloids Surf. B. Biointerfaces.* 36 (2004) 81–90.
- [28] J.H. Merritt, D.E. Kadouri, G.A. O'Toole, Growing and Analyzing Static Biofilms, *Curr. Protoc. Microbiol.* 00:B:1B.1: (2005).
- [29] A. Roosjen, H.J. Busscher, W. Norde, H.C. van der Mei, Bacterial factors influencing adhesion of *Pseudomonas aeruginosa* strains to a poly(ethylene oxide) brush., *Microbiology.* 152 (2006) 2673–82.
- [30] D. Verrier, B. Mortier, G. Albagnac, Initial adhesion of methanogenic bacteria to polymers, *Biotechnol. Lett.* 9 (1987) 735–740.
- [31] J.M. Sanchez, S. Arijó, M. a. Muñoz, M. a. Morinigo, J.J. Borrego, Microbial colonization of different support materials used to enhance the methanogenic process, *Appl. Microbiol. Biotechnol.* 41 (1994) 480–486.
- [32] C.J. van Oss, Acid—base interfacial interactions in aqueous media, *Colloids Surfaces A Physicochem. Eng. Asp.* 78 (1993) 1–49.
- [33] H. Busscher, A.H. Werkamp, Specific and non-specific interactions in bacterial adhesion to solid substrata, *FEMS Microbiol. Rev.* 46 (1987) 165–173.
- [34] G. Hwang, S. Kang, M.G. El-Din, Y. Liu, Impact of conditioning films on the initial adhesion of *Burkholderia cepacia*., *Colloids Surf. B. Biointerfaces.* 91 (2012) 181–8.
- [35] M.M.T. Khan, L.K. Ista, G.P. Lopez, A.J. Schuler, Experimental and theoretical examination of surface energy and adhesion of nitrifying and heterotrophic bacteria using self-assembled monolayers., *Environ. Sci. Technol.* 45 (2011) 1055–60.
- [36] H. Wang, M. Sodagari, Y. Chen, X. He, B.Z. Newby, L.-K. Ju, Initial bacterial attachment in slow flowing systems: effects of cell and substrate surface properties., *Colloids Surf. B. Biointerfaces.* 87 (2011) 415–22.
- [37] N. Cerca, G.B. Pier, M. Vilanova, R. Oliveira, J. Azeredo, Quantitative analysis of adhesion and biofilm formation on hydrophilic and hydrophobic surfaces of clinical isolates of *Staphylococcus epidermidis*, *Res. Microbiol.* 156 (2005) 506–514.
- [38] N.P. Boks, W. Norde, H.C. van der Mei, H.J. Busscher, Forces involved in bacterial adhesion to hydrophilic and hydrophobic surfaces, *Microbiology.* 154 (2008) 3122–3133.
- [39] N. Fernández, E.E. Díaz, R. Amils, J.L. Sanz, Analysis of microbial community during biofilm development in an anaerobic wastewater treatment reactor., *Microb. Ecol.* 56 (2008) 121–32.
- [40] S. Langer, D. Schropp, F.R. Bengelsdorf, M. Othman, M. Kazda, Dynamics of biofilm formation during anaerobic digestion of organic waste., *Anaerobe.* 29 (2014) 44–51.

- [41] H.Y. Cheung, S.Q. Sun, B. Sreedhar, W.M. Ching, P. a. Tanner, Alterations in extracellular substances during the biofilm development of *Pseudomonas aeruginosa* on aluminium plates, *J. Appl. Microbiol.* 89 (2000) 100–106.

Table 1. Contact angles, hydrophobicity, surface free energy components and zeta potential measurements of *M. barkeri* and support materials (100 mM, pH 7 potassium chloride). Error values represent standard deviations of 3 independent experiments.

Surface	Contact angle (degrees)			Surface free energy ( $\text{mJ}\cdot\text{m}^{-2}$ )					Zeta potential (mV)
	Water	Diiodomethane	Formamide	$\gamma^{\text{LW}}$	$\gamma^{\text{AB}}$	$\gamma^+$	$\gamma^-$	$\gamma^{\text{total}}$	
<i>M. barkeri</i>	8±2	47±5	9±1	36	21.4	2.12	54	57	-20±3
PE	77±9	42±4	59±1	39	0.75	0.02	9	39	-20±5
PP	91±7	42±3	67±3	39	0.40	0.02	3	39	-12±3
PVC	72±6	29±5	58±3	45	3.39	0.21	14	48	-5±3
PETG	76±1	36±5	60±1	42	1.80	0.08	11	44	-11±5
PVDF	77±6	46±3	64±4	36	1.00	0.02	11	37	-39±4
PTFE	116±2	63±8	81±7	27	1.15	0.23	1	28	-6±5

Figure 1  
[Click here to download high resolution image](#)

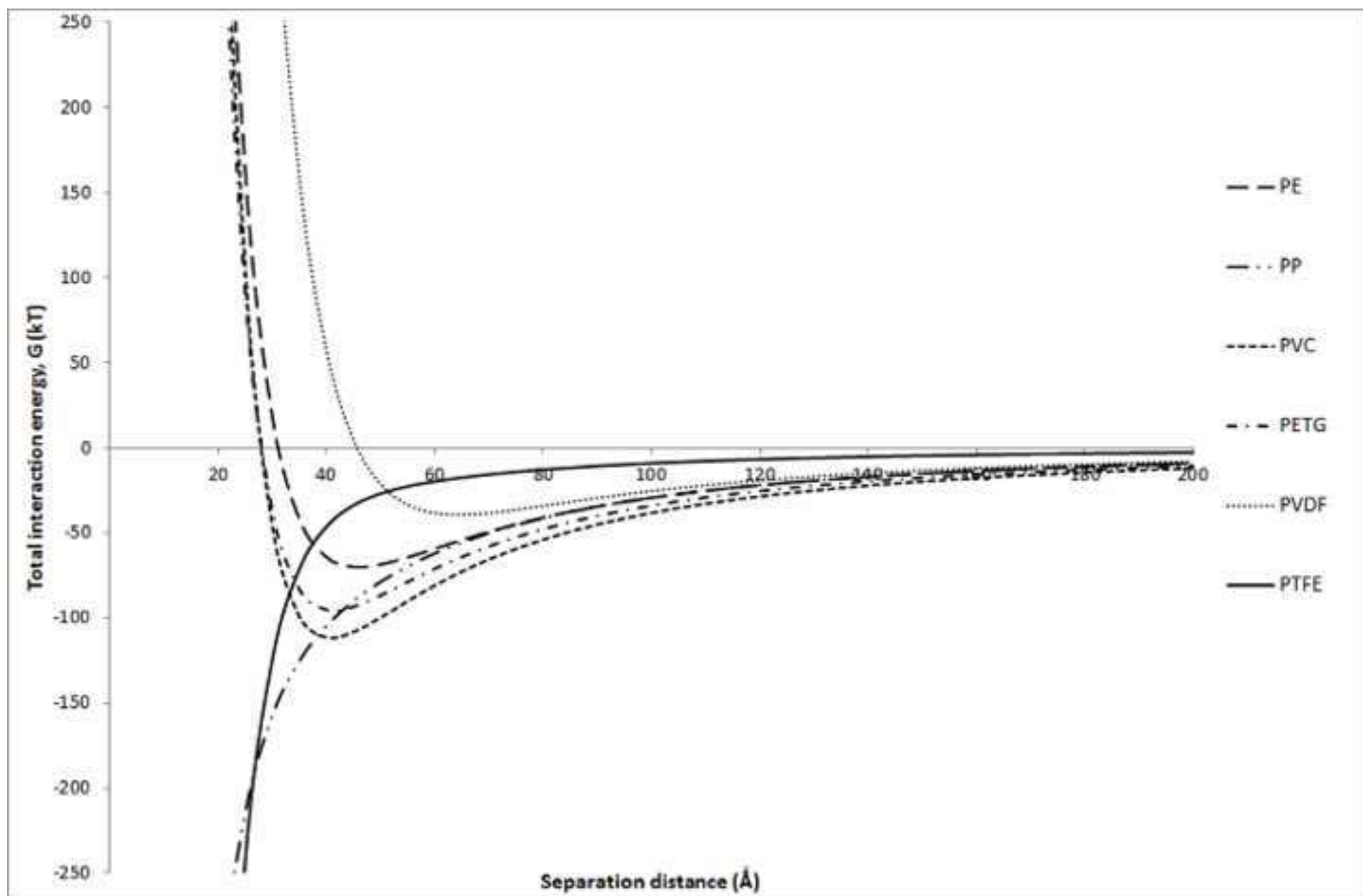
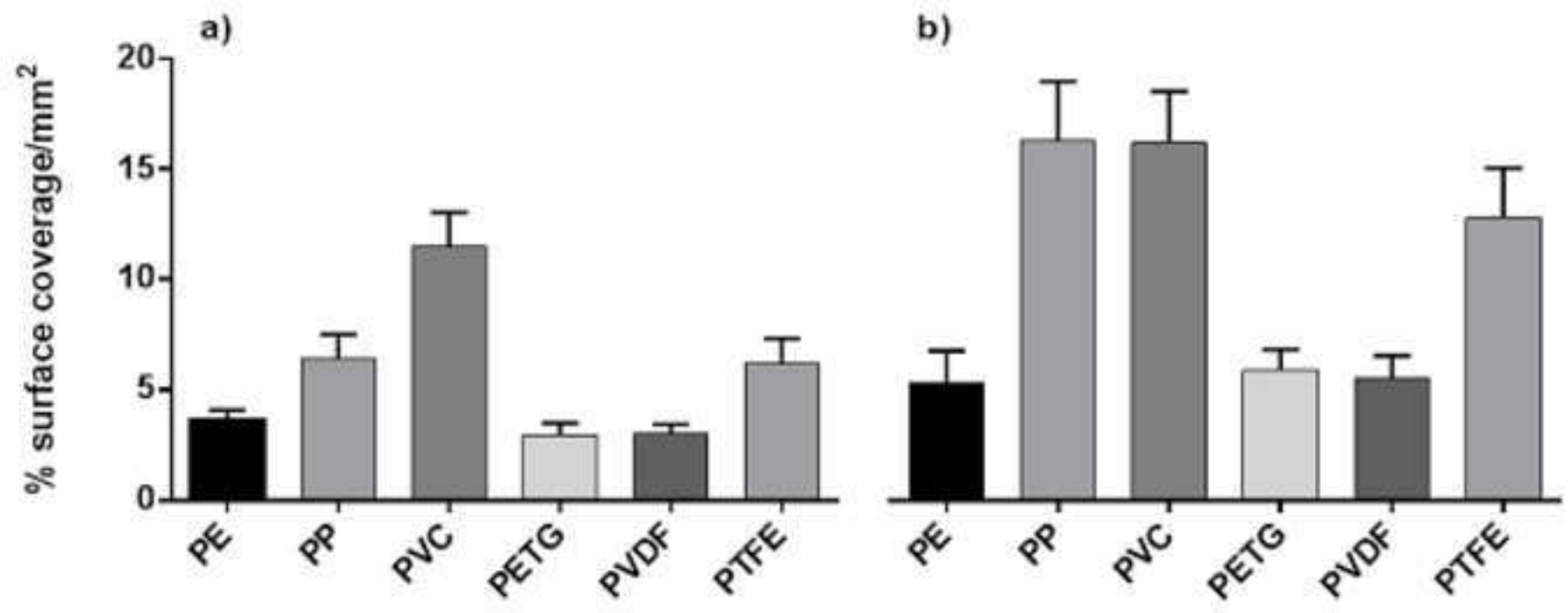


Figure 2  
[Click here to download high resolution image](#)



**Figure 3**  
[Click here to download high resolution image](#)

